

# Analysis and Control of Axial Thrust in Centrifugal Pump by Use of J-Groove

<b>Heishiro ABE</b>	Yokohama National Univ., Japan	heishiro@mach.me.ynu.ac.jp
<b>Kazunari MATSUMOTO</b>	Tatsuno Corporation, Japan	kamatsumoto@tatsuno.co.jp
<b>Junichi KUROKAWA</b>	Yokohama National Univ., Japan	kuro@post.me.ynu.ac.jp
<b>Jun MATSUI</b>	Yokohama National Univ., Japan	jmat@ynu.ac.jp
<b>Young-Do CHOI</b>	Yokohama National Univ., Japan	ydchoi@mach.me.ynu.ac.jp

**Key words:** Centrifugal Pump, Axial Thrust, J-Groove, Thrust Balancing Device, Boundary layer

## Abstract

In order to control and balance axial thrust of turbo machine, many types of balancing devices are used but most of them are complicated and sometimes cause troubles. In this study, a very simple device of using shallow grooves mounted on a casing wall, known as “J-Groove”, is proposed and studied experimentally and theoretically. The result shows that 70% of axial thrust in an industrial 4-stage centrifugal pump can be reduced at the best efficiency point. Moreover, the analytical method of “interfered gap flow” is established and a simple formula which can determine the optimum dimension of groove and its location is proposed.

## Introduction

In order to balance axial thrust of turbo-machines, many devices such as balancing disk, balancing drum, balancing hole and sealing system are used. However, many of these devices become complicated and cause problems such as the vibration by balancing disk. Therefore, a very simple device to balance axial thrust is strongly desired.

Kurokawa et al. have verified that a number of radial shallow grooves mounted on a casing wall can drastically decrease axial thrust (Ref 1). As shown in Fig.1, “J-Groove”, with only 1 or several mm of depth, can drastically decrease the swirl strength in the axial gap flow between an impeller shroud and a casing wall. By this swirl decreasing effect, the radial pressure distribution curve is flattened and the axial thrust is considerably reduced.

This study is intended to apply this simple device to control axial thrust of multi-stage centrifugal pump and examine the effectiveness of J-Groove. Also, this study proposes a simple calculation method to determine the optimum dimension of groove and its location to balance axial thrust without using any other balancing devices.

When grooves are mounted on a casing wall, a strong radial outflow appears in the axial gap.

However, in the case of the strong radial outflow in a very narrow gap, a proper flow model to express the flow field is not established yet. This study will develop a new calculation model for “a narrow gap flow”. With this new model, this study will develop a calculation method to deal with every type of flow from narrow to wide gap flow.

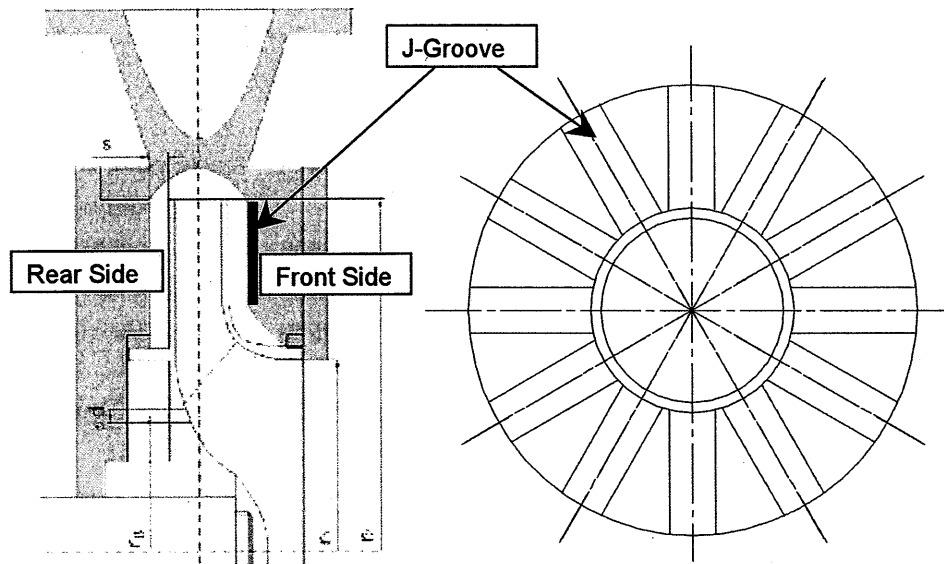


**Fig. 1 Illustration of J-Groove installed on the front wall of pump casing**

### **Theoretical analysis**

The pressure acting on the impeller shroud causes axial thrust. Therefore, axial thrust analysis consists of flow analysis in the gap between a rotating and a stationary wall and the determination of boundary values. Kurokawa et al. have studied with an enclosed rotating disc, which substitutes the flow between the casing wall and the shroud of an impeller (Ref 2). Due to the trend to large size and high speed of centrifugal turbo-machine, a calculation method that covers wide range of Reynolds number is required. Even if CFD-codes are used, it is still difficult to calculate the axial thrust, since the total axial thrust amounts to only a few % of axial force working on the shroud and high accuracy of 0.1% is required. To cover all of these requirements, this study uses the momentum integral method by assuming logarithm law as the velocity profile of the gap flow.

In the gap flow there are generally the following two types. One is the “non-interfered gap flow” which has been widely used in many cases, and the other the “interfered gap flow”, shown in Figs.2 and 3. In the former, the flow consists of the boundary layers on both walls and the core flow in which the tangential velocity  $u$  is expressed as  $Kr\omega$  and no radial flow exist. But in the latter, the core flow disappears and the boundary layers interfere with each other. The interfered gap flow usually exists when the gap is very narrow or/and radial outflow is superimposed, and can be seen in the rear side of a multi-stage centrifugal pump or in the cooling device of a turbine rotor.

In both types of flow, the flow characteristics are determined from the equations of

momentum, angular momentum and continuity shown in the followings;

$$\frac{\partial}{\partial r} r \int_0^s v^2 dz - \int_0^s u^2 dz = -\frac{r}{\rho} \frac{\partial p}{\partial r} s - \frac{r}{\rho} (\tau_{s\theta} + \tau_{r\theta}) \quad (1)$$

$$\frac{\partial}{\partial r} \int_0^s r^2 u v dz = -\frac{r^2}{\rho} (\tau_{s\theta} + \tau_{r\theta}) \quad (2)$$

$$\int_0^\theta v dz + \int_0^\delta v' dz' = \frac{Q_i}{2\pi r} \quad (3)$$

where  $r$  and  $z$  are radial and axial distances, respectively,  $u$  and  $v$  are tangential and radial velocities,  $p$  is pressure,  $\rho$  is density of fluid,  $\tau_r$  and  $\tau_s$  are wall shearing stresses of rotating and stationary walls, respectively.  $Q_i$  is through flow rate in the axial gap, and  $Q_i > 0$  when outflow is superposed. Subscripts  $r$  and  $\theta$  are radial and tangential components, respectively.

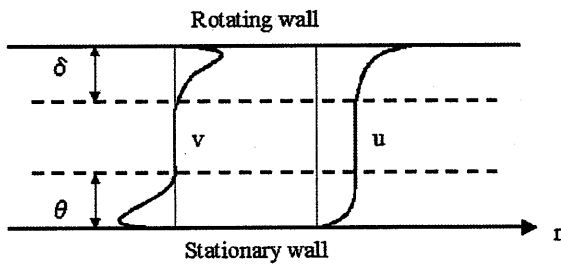


Fig. 2 Non-interfered gap flow model

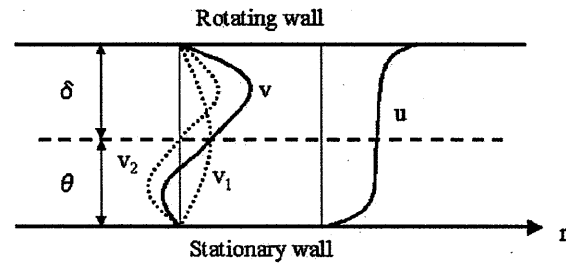


Fig. 3 Interfered gap flow model

### Theory of non-interfered gap flow

As shown in the above, the non-interfered gap flow consists of the boundary layers on both walls assuming the followings;

- i. The core flow existing between 2 boundary layers has a tangential velocity  $u$  expressed as  $Kr\omega$  and no radial flow.
- ii. The velocity distribution in the boundary layer on the stationary wall is expressed as below:

$$\frac{u}{v_*} = \phi(\eta) \quad (4)$$

$$\frac{v}{v_*} = -a \left(1 - \frac{\eta}{\eta_1}\right) \phi(\eta) \quad (5)$$

- iii. The velocity distribution in the boundary layer on the rotating wall (denoted by dash (')) is expressed as below:

$$\frac{u'}{v'_*} = \frac{r\omega}{v'_*} - \phi(\zeta) \quad (6)$$

$$\frac{v'}{v'_*} = a' \left(1 - \frac{\zeta}{\zeta_1}\right) \phi(\zeta) \quad (7)$$

where  $\eta \equiv \frac{v_* z}{\nu}$ ,  $\zeta \equiv \frac{v'_* z'}{\nu}$ ,  $u = u' = Kr\omega$  (at  $\eta = \eta_1 \equiv \frac{v_* \theta}{\nu}$  and  $\zeta = \zeta_1 \equiv \frac{v'_* \delta}{\nu}$ ) and

$\phi(\xi) \equiv 2.5 \ln(9.0\xi + 1)$  are defined as so.

From the Daily's equation of boundary layer thickness on the rotating disk,

$$\delta = \frac{0.400(1-K)^2 r}{(\omega r^2/\nu)^{1/5}} \quad (\text{Ref 3}) \quad (8)$$

When equations (4) to (8) are inserted into equations (2) and (3), tangential velocity ratio  $K$  can be determined by an ordinary differential equation on  $R$  ( $\equiv r/r_2$ ) as below.

$$f_1(K, R, C_q) \frac{dK}{dR} = f_2(K, R, C_q) \quad (9)$$

where  $C_q$  is the nondimensional through flow rate and is defined as  $C_q = Q_i / 2\pi r_2^3 \omega$ .

### Theory of interfered gap flow

In an interfered gap flow the core flow disappears and the boundary layers interfere with each other that are caused by a very narrow gap or/and radial outflow. The following assumption is adopted for the calculation of the flow.

- i. The boundary layers interfere at center of the gap and its tangential velocity is  $Kr\omega$ .
- ii. The velocity distribution on the side of stationary wall is expressed as below:

$$\frac{u}{v_*} = \phi(\eta) \quad (10)$$

$$\frac{v}{v_*} = -a(1 - \frac{\eta}{\eta_1})\phi(\eta) + b \frac{\phi(\eta)}{\phi(\eta_1)} \quad (11)$$

- iii. The velocity distribution on the side of rotating wall is expressed as below:

$$\frac{u'}{v'_*} = \frac{r\omega}{v'_*} - \phi(\zeta) \quad (12)$$

$$\frac{v'}{v'_*} = a'(1 - \frac{\zeta}{\zeta_1})\phi(\zeta) + b' \frac{\phi(\zeta)}{\phi(\zeta_1)} \quad (13)$$

where  $\eta \equiv \frac{v_* z}{\nu}$ ,  $\zeta \equiv \frac{v'_* z'}{\nu}$ ,  $u = u' = Kr\omega$  (at  $\eta = \eta_1$  and  $\zeta = \zeta_1$ ) and  $\phi(\xi) \equiv 2.5 \ln(9.0\xi + 1)$  are defined as so.

When above equations are inserted into equations (2) and (3),  $K$  can be determined by an ordinary differential equation on  $R$  as below.

$$f_3(K, R, C_q) \frac{dK}{dR} = f_4(K, R, C_q) \quad (14)$$

### Theory in the case of J-Groove installed on the casing wall

When the J-Groove is installed on the casing wall, the radial inward flow is induced in the shallow groove due to the pressure gradient. The groove flow makes the outward flow along a rotating disk increase to satisfy the equation of continuity, that is

$$\int_0^\theta v dz + \int_0^\theta v' dz = Q_l + Q_G \quad (15)$$

where  $Q_l$  and  $Q_G$  are radial through flow rate in the axial gap between rotating disk and stationary casing wall and the flow rate in the grooves, respectively.

The groove flow is determined by the radial balance as below.

$$\tau_r dr = 4r_h dp \tag{16}$$

where  $\tau_r$  and  $r_h$  are shear stress to radial direction and hydraulic radius of the groove, respectively.

**Determination of pressure distribution and axial thrust**

From equation (1), pressure distribution can be determined as below.

$$\frac{dC_p}{dR} = 2K^2 R + 2R \left( \frac{C_q}{R^2 S} \right)^2 \tag{17}$$

where  $C_p$  is defined as  $C_p = (p - p_2) / \left( \frac{\rho}{2} r_2^2 \omega^2 \right)$  ( $p_2$  is the pressure at  $r=r_2$ .) and  $S$  is gap ratio defined as  $S = s/r_2$ .

The axial force working on each side of the impeller can be determined by integrating the pressure distribution as below.

$$F = \int_{r_i}^{r_2} 2\pi r p(r) dr = C_F \cdot \rho \pi r_2^4 \omega^2 \tag{18}$$

where  $r_i$  and  $r_2$  are the inner and outer radius of impeller, respectively, and  $C_F$  is the axial force coefficient.

The total axial thrust  $T$  is given by the difference of axial forces  $F_F$ ,  $F_R$  on front and rear shroud and momentum change of the inlet flow working on the impeller as below.

$$T = F_R - F_F - \rho Q v \tag{19}$$

where  $Q$  [m<sup>3</sup>/s] is main flow rate and  $v$  [m/s] is flow velocity at the mouth of impeller.

**Evaluation of the interfered gap flow model.**

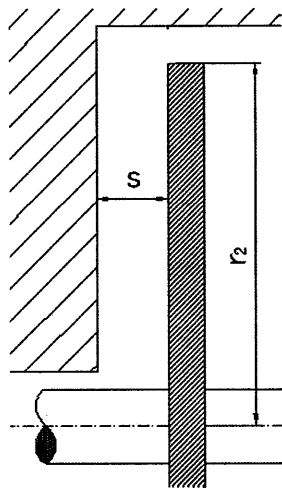


**Fig. 4 Rotating disk model**

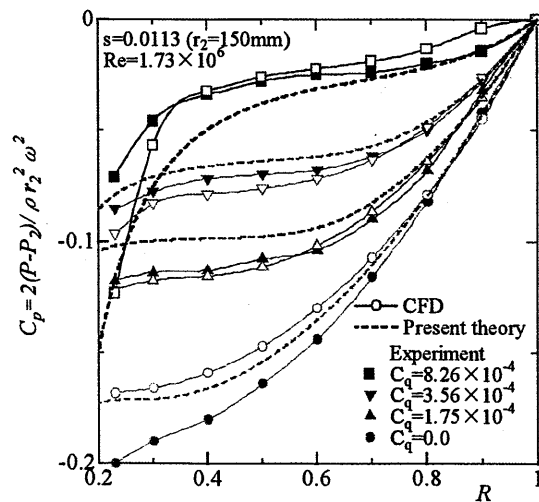


**Fig. 5 Comparison of pressure distribution**

In order to confirm the validity and reliability of present theoretical analysis, comparison is conducted among the results from the present theoretical analysis, CFD calculation by use of commercial code ANSYS CFX and experiment using the enclosed rotating disc model as shown in Fig. 4. In the case of CFD calculation when radial outflow is imposed on a very narrow gap flow, the result of CFD calculation is hardly converged because tangential velocity becomes almost zero. Therefore, present CFD and experimental conditions in Fig. 5 are determined in consideration of a limit convergence range of CFD calculation by the rate of axial gap versus flow rate of radial outflow. The momentum integral method (using “interfered gap flow model”) and a  $k-\omega$  model in the CFD calculation are compared in Fig. 5 where the radial pressure distributions in a narrow gap along an enclosed rotating disk with superimposed radial flow are compared. Figure 5 reveals that the present theory (momentum integral method), CFD ( $k-\omega$  model) and experiment (Daily et al., Ref 3) agree well each other.

### Test pump and reduction of axial thrust by J-Groove

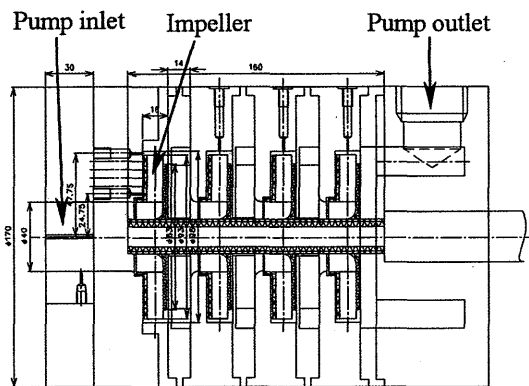


Fig. 6 4-stage centrifugal pump tested

Figure 6 shows an industrial 4-stage centrifugal pump tested. Specific speed of the pump is  $n_s=256$  [ $\text{min}^{-1}$ ,  $\text{m}^3/\text{min}$ ,  $\text{m}$ ]. The radius of impeller  $r_2$  is 46.5mm and there is a cut at  $R (=r/r_2)=0.892$  of rear shroud. The impeller has 6 blades and the blade outlet angle is  $22.5^\circ$ . J-Groove is mounted on the casing wall and its dimension is depth  $d=1\text{mm}$   $\times$  width  $w=10\text{mm}$   $\times$  length  $l=26.75\text{mm}$  and numbers  $n=0$  to 12.

Maximum efficiency of the test pump does not change by the installation of J-Groove as shown in Fig. 7. However, by installation of J-Groove, axial thrust is reduced

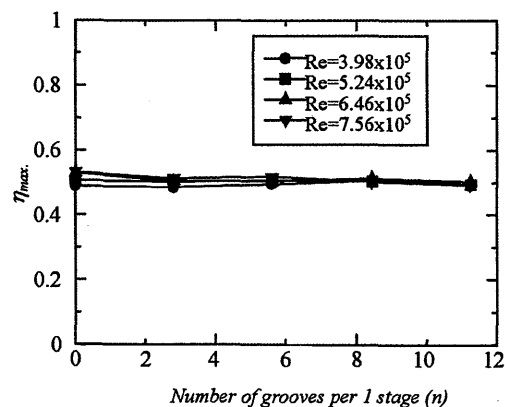


Fig. 7 Maximum efficiency vs. number of grooves

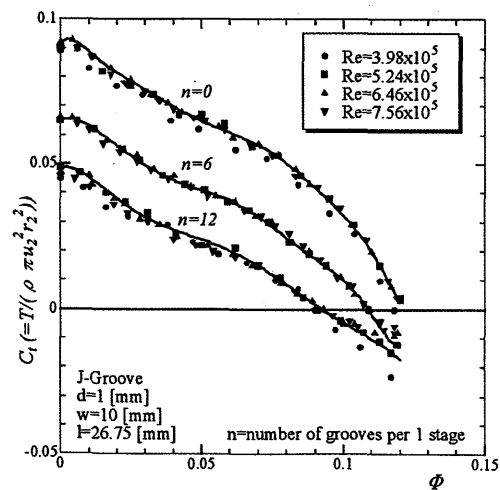
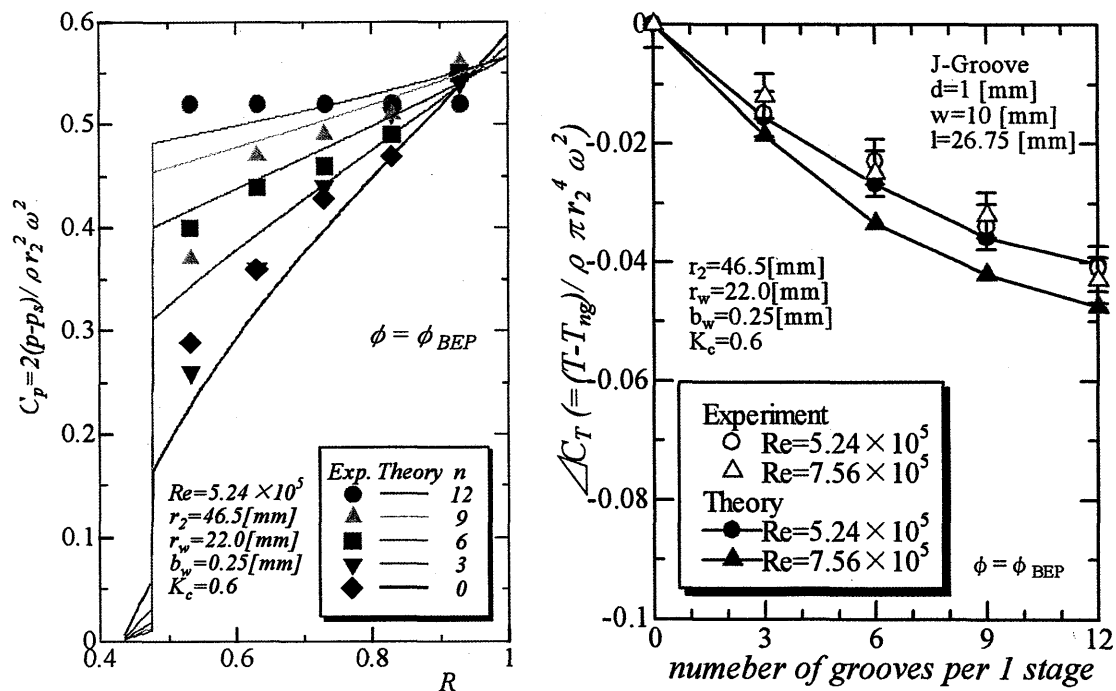


Fig. 8 Decrease of axial thrust by J-Groove

considerably in the all flow rate ranges and similarity law is kept even with the use of J-Groove as shown in Fig. 8. Especially, in the case of groove number of  $n=12$ , axial thrust decreases considerably. It is seen that the axial thrust at the best efficiency point ( $\phi=0.067$ ) drops by 70%.

### Effect of J-Groove and its optimum dimension

The predicted distributions of pressure coefficient  $C_p$  in the front gap of the test pump and axial thrust reduction  $\Delta C_T$  by use of J-Groove are compared with the experimental results in Fig. 9. Non-interfered gap flow model is adopted for the theoretical analysis, as the present theory revealed that the inward leakage flow rate is very large in the front shroud gap. A large inward flow is induced in the groove, resulting a large outward flow in the axial gap to satisfy the equation of continuity. Therefore, tangential velocity decreases remarkably and the radial pressure gradient becomes gradual. Theoretical results correspond to those of the experiment well.



(a) Pressure coefficient  $C_p$  vs. radius ratio  $R (=r/r_2)$  (b) Reduction ratio  $\Delta C_T$  vs. number of J-Groove  
**Fig. 9 Comparison of theory with experiment**

In order to determine the optimum dimensions of J-Groove, many calculations were performed by changing the parameters of pump dimensions and groove dimensions. The calculated results revealed that the effect of all parameters on axial thrust can be represented by one parameter, that is *TC No.* defined as follows. The *TC No.* is derived by the multiplication of *JE No.* (Ref 4) and the results of many calculations for the parameters.

$$TC\ No. = n(DW)^{12/7} (2D + W)^{-5/7} L^{1/5} (1 - R_w)^3 B_w^{2/5} C_{pc} K_c^2 Re^{1/4} \quad (20)$$

where  $D = d/r_2$ ,  $W = w/r_2$ ,  $L = l/r_2$ ,  $R_w = r_w/r_2$  (wearing ring radius),  $B_w = b/r_2$  (wearing ring

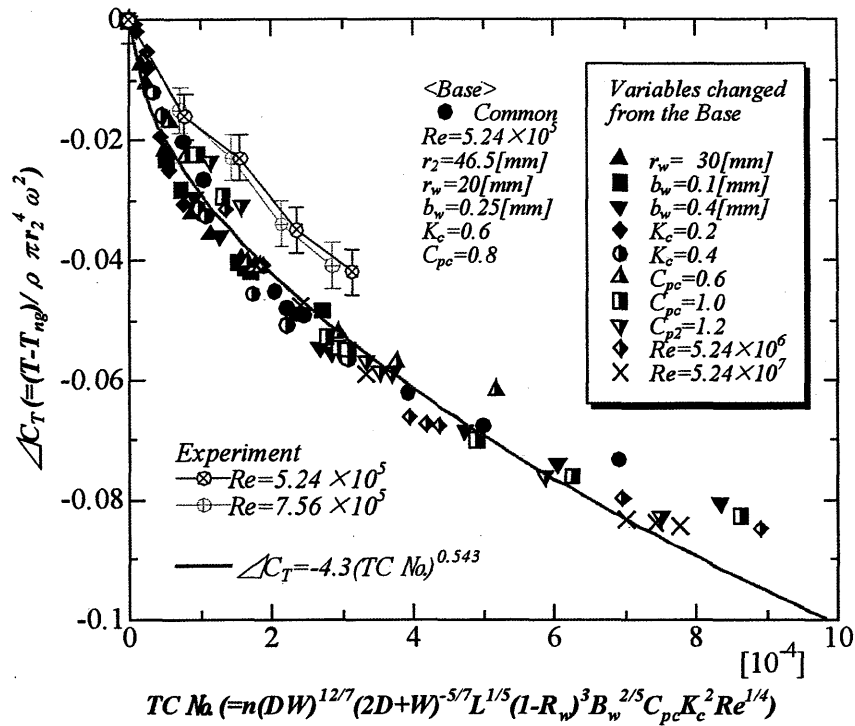


Fig. 10 Axial thrust reduction vs.  $TC No.$

clearance), and  $C_{pc} = 2p^2 / \rho r_2^2 \omega^2$  and  $K_c = v_{\theta 2} / r_2 \omega$  are the pressure coefficient and tangential velocity ratio at the impeller outlet, respectively.

All the results are summarized in in Fig.10, which is applicable to any types of centrifugal pump and any J-Groove dimensions. Ordinate represents the differential thrust defined as

$\Delta C_T = (T - T_{ng}) / \rho \pi r_2^4 \omega^2$  where  $T_{ng}$  is the value of thrust in the case of no J-Groove, and

abscissa reveals  $TC No.$  which considers the effect of the dimension of groove, wearing ring, impeller outlet boundary conditions and the Reynolds number. The figure shows that 1 curvilinear line can be drawn through the plots of every different condition. This curvilinear line is plotted using the equation (21) to determine the optimum dimension of groove to balance axial thrust under any condition.

$$\Delta C_T = -4.3 (TC No.)^{0.543} \tag{21}$$

While, there is a limitation of the above equation for every condition, because the outlet pressure of impeller can't be lower than the inner pressure, which means that completely flat distribution will be the limit. This critical value of axial thrust reduction,  $C_{Tcr}$ , which is derived by multiplication of the results of many calculations performed by changing the parameters of pump dimensions, is given by the following formula ;

$$\Delta C_{Tcr} = 0.0318 (1 - R_w)^{0.6} C_{pc}^{0.6} K_c^{0.6} Re^{0.02} C_q^{-0.2} \tag{22}$$

By using these equations, it is possible to determine the optimum dimension of J-Groove and the limitation of the  $\Delta C_T$  value to balance the axial thrust of a centrifugal pump.



In addition, the differential axial thrust( $\Delta C_T$ ) increases as the leakage( $\Delta C_q$ ) increases too. The equation to determine the rate of  $\Delta C_q$  per  $\Delta C_T$  is shown as below. Moreover, the correlation is shown in Fig. 11.

$$\Delta C_q / \Delta C_T = 0.851(1 - R_w)^{-1.2} B_w^{1.2} C_{pc}^{-0.5} K_c^{-0.2} Re^{0.07} \quad (23)$$

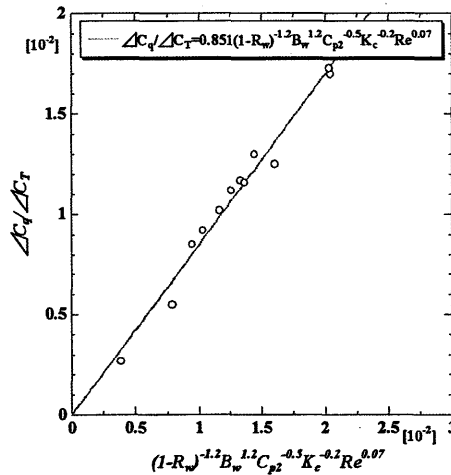


Fig. 11 The rate of  $\Delta C_q$  per  $\Delta C_T$

## Conclusions

1. J-Groove attached on the front casing wall of an industrial 4-stage centrifugal pump reduced axial thrust considerably over the whole flow rate range. At the best efficiency point, 70% of axial thrust is reduced. Present theory predicts the groove effect well.
2. Present theory predicts the pressure distribution of gap flow imposed with radial through flow well from a very narrow gap to a wide gap.
3. A guideline for optimum configurations of J-Groove is proposed using a simple calculation method which considers the effect of the dimensions of groove, wearing ring, boundary conditions of impeller outlet and Reynolds number to balance the axial thrust.

## References

- Ref 1 Kurokawa, J., Kamijo, K. and Shimura, T., "Axial Thrust Behavior in LOX-Pump of Rocket Engine," AIAA Journal of Propulsion and Power, Vol. 10, No. 2, pp. 244-250, 1994.
- Ref 2 Kurokawa, J. and Sakuma M., "Flow in a Narrow Gap Along an Enclosed Rotating Disk with Through-Flow," JSME International Journal, Vol. 31, No. 2, pp. 243-251, 1988.
- Ref 3 Daily, J. W., Ernst, W. D. and Asbedin, V.V., "Enclosed rotating Disk with Superimposed Through-Flow," MIT Hydro. Lab. Report, No. 64, 1964.
- Ref 4 Saha, S. L., Kurokawa, J., Matsui, J. and Imamura, H., "Suppression of Performance Curve Instability of a Mixed Flow Pump by Use of J-groove," ASME Journal of Fluids Engineering, Vol. 122, pp. 592-597, 2000.